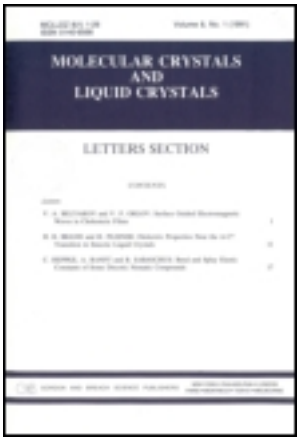

Molecular Crystals and Liquid Crystals
Publication details, including instructions for authors and subscription information:
http://www.tandfonline.com/loi/gmcl20

Thermal Annealing Effects on the Characteristics of Transparent Semiconducting Zn_2SnO_4 Thin Films Prepared by RF-Magnetron Sputtering with Powder Target

Gyo Jung Lee [a] , Do Kyung Lee [b] & Sang Ho Sohn [a]
[a] Department of Physics , Kyungpook National University , Daegu , 702-701 , Korea
[b] Department of Advanced Energy Material Science and Engineering , Catholic University of Daegu , Gyeonsan , Gyeongsangbuk-do , 712-702 , Korea
Published online: 08 Jan 2014.

To cite this article: Gyo Jung Lee , Do Kyung Lee & Sang Ho Sohn (2013) Thermal Annealing Effects on the Characteristics of Transparent Semiconducting Zn_2SnO_4 Thin Films Prepared by RF-Magnetron Sputtering with Powder Target, Molecular Crystals and Liquid Crystals, 586:1, 179-187, DOI: 10.1080/15421406.2013.853552

To link to this article: http://dx.doi.org/10.1080/15421406.2013.853552

Mol. Cryst. Liq. Cryst., Vol. 586: pp. 179–187, 2013

ISSN: 1542-1406 print/1563-5287 online
DOI: 10.1080/15421406.2013.853552

Taylor & Francis
Taylor & Francis Group

Thermal Annealing Effects on the Characteristics of Transparent Semiconducting Zn_2SnO_4 Thin Films Prepared by RF-Magnetron Sputtering with Powder Target

GYO JUNG LEE,[1] DO KYUNG LEE,[2,*] AND SANG HO SOHN[1,*]

[1]Department of Physics, Kyungpook National University, Daegu 702-701, Korea
[2]Department of Advanced Energy Material Science and Engineering, Catholic University of Daegu, Gyeonsan, Gyeongsangbuk-do 712-702, Korea

Effects of thermal annealing on the structural, electrical and optical properties of transparent semiconducting Zn_2SnO_4 (ZTO) thin films have been investigated. The ZTO thin film with the thickness of about 100 nm is prepared by the RF-magnetron sputtering technique using powder target. The experimental results show that the ZTO films annealed at above 400 °C possess inverse cubic spinel structure with a preferred grain orientation in the (311) direction. The transmittances of the ZTO films are approximately 80% in visible region regardless annealing temperature. The increasing annealing temperature leads to the increase in Hall mobility and electron concentration, resulting in the decrease of resistivity. The optical band gap of the films increases with the increase of annealing temperature.

Keywords: Powder target; thermal annealing; transparent thin film transistor; transparent semiconducting oxide; Zn_2SnO_4

Introduction

Transparent thin film transistors (TTFTs) with metal oxide semiconductor have attracted much attention for the application of display devices owing to high mobility, low temperature processing, excellent uniformity, and good transparency to visible light [1–5]. In metal oxide-based TTFTs, although the In-based oxide semiconductors exhibit good performances, due to the scarcity and expense of indium, it is needed to develop In-free oxide semiconductor materials for fabrication of cost effective TTFTs. In this context, zinc-tin-oxide (ZTO) is considered as a prominent candidate for In-free semiconductors [6–9].

The high quality of ZTO thin films has been achieved by fabrication of RF-magnetron sputtering method and most of researches used ceramic ZTO as a target material in sputtering [10,11]. However, hot pressed or sintered ceramic targets may have a tendency to crack due to the localized thermal shock induced by the collisions of the energetic particles

*Address correspondence to Prof. Do Kyung Lee, Department of Advanced Energy Material Science and Engineering, Catholic University of Daegu, 13-13 Hayang-ro, Hayang-eup, Gyeongsan-si, Gyeongsangbuk-do 712-702, Korea (ROK). Tel.: (+82) 53-850-2771; Fax: (+82) 53-850-2770, E-mail: dokyung@cu.ac.kr and Prof. Sang Ho Sohn, Department of Physics, Kyungpook National University, 80 Daehak-ro, Buk-gu, Daegu 702-701, Korea (ROK). Tel.: (+82)53-950-5892; Fax: (+82)53-950-6893. E-mail: shsohn@knu.ac.kr

in high-density plasma [12–14]. In addition, a change in the chemical composition on the target surface during the entire fabrication process can cause the non-uniformity of TTFT performances. The use of powder target can be free of target cracking issues since the powder is loosely packed. Moreover, it is relatively cost-effective way because oxide powder itself is sputtered without further treatments such as forming, sintering, and bonding.

In order to get the high-performance TTFTs, ZTO semiconductors have been annealed at temperatures typically over 500 °C [6,7]. Although the characteristics of ZTO-based TTFT compare well with those of the In-based TTFT, comprehensive study for the thermal annealed ZTO film under vacuum ambient is still relatively rare. Furthermore, thermal annealing effects on the properties of powder target-sputtered ZTO films are yet to be reported.

In this study, we have prepared transparent semiconducting ZTO thin film by RF-magnetron sputtering method using powder target, and investigated their structural, electrical and optical properties after thermal annealing treatments.

Experimental

ZTO thin films were deposited on unheated glass substrate by a RF-magnetron sputtering from the compact powder target designed as 3 inch circle. For the preparation of ZTO sputtering target materials, the powder blends were mixed using the appropriate quantities of pure ZnO (High purity chemicals, 99.99%) and SnO_2 (Cerac, 99.995%) powders having a stoichiometric Zn_2SnO_4 composition. The powders were ball-milled together with ethanol for 24 hrs. After drying, the powders were performed by the calcination in an air atmosphere. Details of calcination conditions used to fabricate ZTO powder for the use of sputtering target are as follows. The temperature was increased to 650 °C at a heating rate of 5 °C/min., and then held for 60 min. The temperature was further increased to 1300 °C using a heating rate of 5 °C/min and maintained at that temperature for 180 min. Finally, the furnace was cooled down to room temperature naturally. The structure of calcined powders was examined by X-ray diffraction (XRD, Phillips PW3710) measurement, using Cu-Kα radiation, and its result is shown in Fig. 1. It is found that the XRD pattern of the sputtering power target exhibits inverse cubic spinel structure according to the JCPDS data base of card number 74-2184. The powder was pressed into an Al target holder with 3 inch diameter. The powder in the targets was completely replaced for every deposition. Prior to deposition, glass substrates were cleaned with acetone, methanol and de-ionized water for 10min in an ultrasonic bath. The base pressure in the chamber was adjusted to 3.0×10^{-6} Torr. Then, high purity argon and oxygen gases were introduced into the chamber through mass flow controller. The powder target was presputtered in Ar and O_2 gas mixture for 5 min. to clean the target surface for enhanced film qualities. ZTO thin film with a thickness of about 100 nm was prepared by sputtering at an applied RF power of 100 W with an Ar/O_2 ratio of 9:1 and the gas pressure of 2 mTorr. ZTO thin films prepared in this way were annealed in vacuum furnace with varying temperatures ranging from 300 °C to 500 °C for a period of 1 hr under the high vacuum of 5.0×0^{-5} Torr.

Film thickness was measured by a surface profiler (KLA Tencor, Alpha-Step IQ) and confirmed by the cross-sectional images of a field emission scanning electron microscope (FE-SEM, Hitachi S4200). The structural characterizations of the as-deposited and annealed ZTO thin films were carried out using XRD techniques. The surface microstructure of the films was analyzed using the FE-SEM observation. The electrical properties of the films were obtained from the Hall Effect measurement (Ecopia, HMS-3000) using a Van

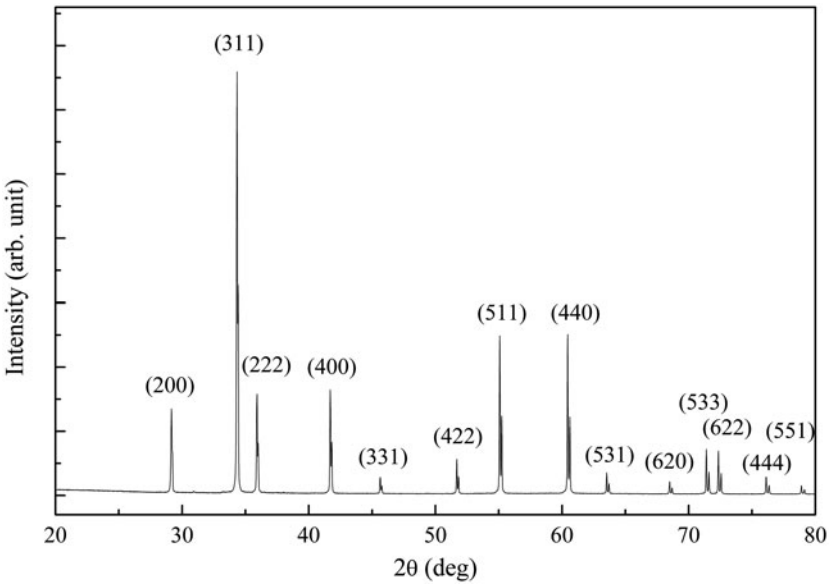

Figure 1. XRD pattern of the prepared ZTO powder for the use of sputtering target.

der Pauw technique. Optical characteristics of the films were measured by means of an ultraviolet-visible-infrared spectrophotometer (Varian, Cary 5G) in the wavelength range of 250∼2500 nm. All measurements were carried out at room temperature.

Results and Discussion

Figure 2 shows the XRD patterns for ZTO thin films annealed at different temperatures between 300 °C to 500 °C with interval of 100 °C for 1 hr. For reference, the XRD pattern of as-grown ZTO thin film is also indicated. It can be observed that no significant phase existed for the as-grown film and the film annealed at 300 °C, indicating an amorphous state. For the films annealed at 400 °C and 500 °C, the main peak can be observed at about $2\theta = 34^{\circ}$, which is a preferred (311) orientation in the inverse cubic spinel structure. It is also coincided with the XRD pattern of powder target, as shown in Fig. 1. Consequently, the thermal annealing treatment at temperature over 400 °C results in the crystallization of the ZTO films due to the sufficient activation energy for the atoms to diffuse. It is interesting to note that the intensity of (311) peak for the film annealed at 400 °C is relatively low and broad, indicating initial formation of the inverse cubic spinel phase. At higher annealing temperature, the smaller full width half maximum and higher intensity of the peak can be seen in the pattern, representing the enhancement of the film crystallinity.

Figure 3 indicates FE-SEM images on the surface of ZTO thin films as a function of annealing temperature. It has been found that in Figs. 3(a) and (b), the surfaces of as-grown and 300 °C-annealed films are very smooth and featureless without defects such as pinholes, voids and visible cracks. In addition, there are neither crystallites nor grain boundary. These features reflect the amorphous nature of the ZTO film. When annealing temperature is raised up at 400 °C, the grains are distributed with amorphous zone over the film surface. We can see the densely arranged grains on the surface for an annealing temperature of 500 °C, as shown in Figure 3(d). These can be explained by that the thermal

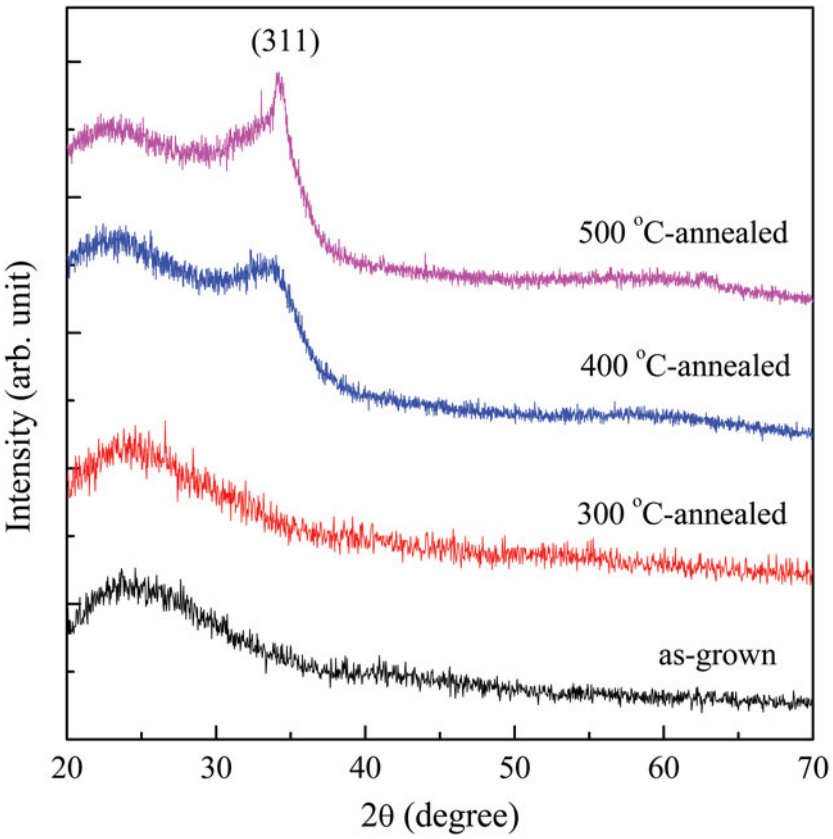

Figure 2. XRD patterns for ZTO films annealed at temperatures ranging from 300 to 500.

energy allows the rearrangement of atoms in the film to create crystallization and grain growth, which is accordant with the XRD examination results of the films.

Figure 4 presents the electrical resistivity, Hall mobility and carrier concentration of all the ZTO thin films. It is seen from Fig. 4 that with an increasing annealing temperature, the resistivity of the films decreases while the mobility and carrier concentration increase. It is known that the resistivity is proportional to the reciprocal of the product of the carrier concentration and the mobility. Accordingly, the variation in the resistivity of the ZTO films with annealing temperature is attributed to the changes in the mobility and carrier concentration. The mobility of the ZTO film is shown to be increased with increasing annealing temperature. The dependence of the mobility on the annealing temperature can be explained by the improved crystallinity of the film. In general, the electron mobility in crystalline oxide is superior to that of amorphous. Also, the electron transport in crystalline oxide is governed mainly by the scattering at the grain boundaries, and hence the grain size is the main factor for the mobility. From the results of XRD and FE-SEM observations, the grain size increases with the increasing annealing temperature. Therefore, the higher mobility of the ZTO film at a higher annealing temperature may be originated in the decrease of the grain boundary scattering. The enlargement of carrier concentration with the increase of annealing temperature can be attributed to the enhancement of oxygen release at higher annealing temperature. It can be generally accepted that the carrier concentration is

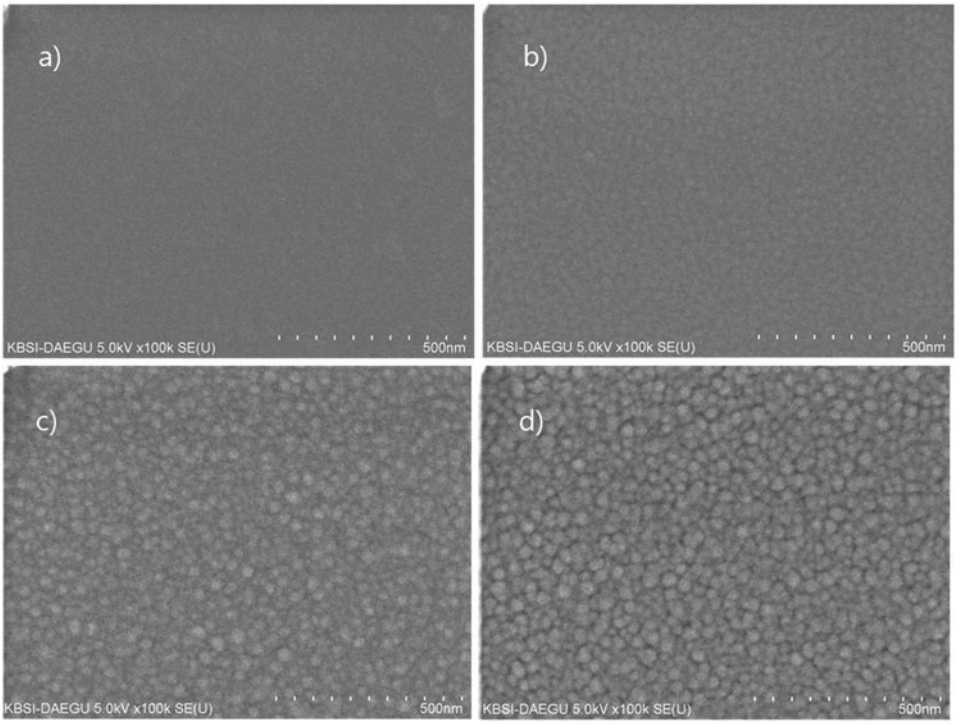

Figure 3. FE-SEM images on the surface of ZTO films annealed at different temperatures. (a) as-grown, (b) 300 °C-annealed, (c) 400 °C-annealed, and (d) 500 °C-annealed

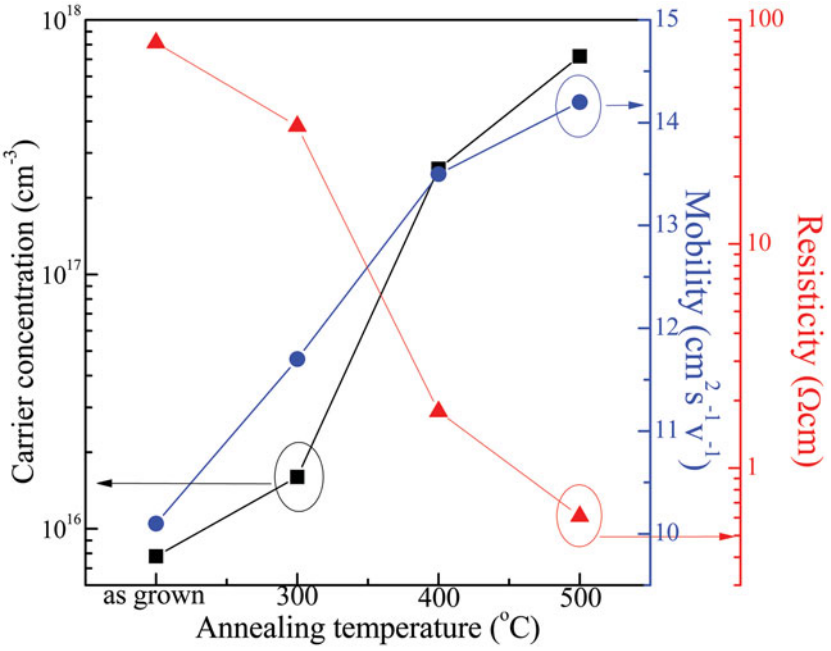

Figure 4. Dependence of electrical properties of ZTO thin films on the annealing temperature.

originated from the oxygen vacancies. During vacuum annealing process, the generation of oxygen vacancies can be occurred due to supplied thermal energy [15]. From the viewpoint of TTFT application, it is worth noting that the resistivity of the ZTO films annealed at 400 °C and 500 °C is about 1.79 Ωcm and 0.61 Ωcm, respectively. These values are within the range of resistivity for usable semiconductor in the TTFT [16]. Furthermore, the 400 °C and 500 °C-annealed ZTO films show the respective mobility of about 13.5 cm^2/Vs and 14.2 cm^2/Vs, which are comparable to that of sputtered IGZO film [17].

The optical transmission spectra of the ZTO films on glass substrate within the wavelength range between 250 and 2500 nm are shown in Fig. 5. The optical transmittance of glass substrate is also measured for reference purpose and has a transmittance of about 91.2% at 550 nm wavelength. As clearly seen in Fig. 5, all annealed films have an average optical transparency over 80% in the visible range, and there is not larger fluctuation in the spectra. In the inserted figure, the transmittance of as-grown ZTO film including the substrate at 550 nm wavelength is observed to be about 82.6%. The optical transmittance of about 78.1% is obtained for the 500 °C-annealed ZTO film. These results indicate that the ZTO films are transparent in the visible region, which indicates good optical characteristics of the channel active layer in TTFT. On the other hand, the UV absorption edge in the spectra is blue-shifted after annealing process, indicating the increasing of the optical band

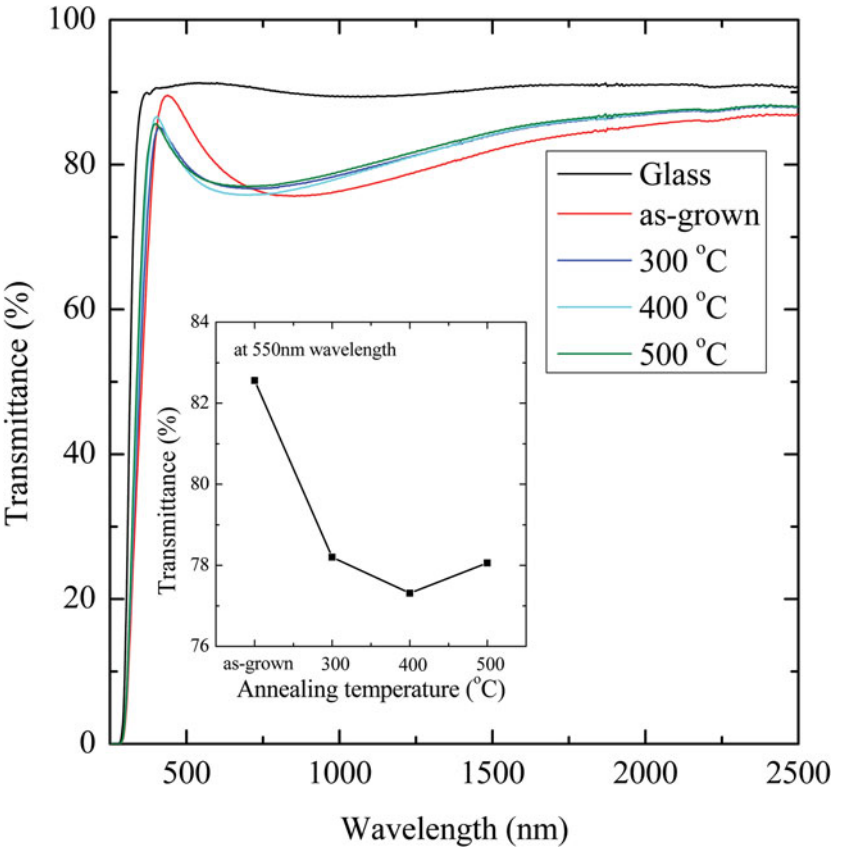

Figure 5. Optical transmittances of the annealed ZTO films.

gap. The optical band gap (E_g) of the films can be determined by the extrapolation methods from absorption edge. The coefficient of absorption (α) is determined by the following equation.

$$\alpha = (1/t)\ln(1/T),$$

where T is the transmittance and t is the film thickness. It has been known that ZTO film is a direct n-type semiconductor. The absorption edge for direct interband transition is given by

$$\alpha h\upsilon = A(h\upsilon - E_g)^{1/2},$$

where A is the constant for a direct transition, h is Planck's constant, and υ is the frequency of the incident photon.

The inserted in Fig. 6 show the graphs of α^2 against photon energy $h\upsilon$ for as-grown and 500 °C-annealed ZTO thin films. The straight-line portion of the curve, when extrapolated to zero, gives the optical band gap E_g. As seen from Fig. 6, E_g value of ZTO thin film

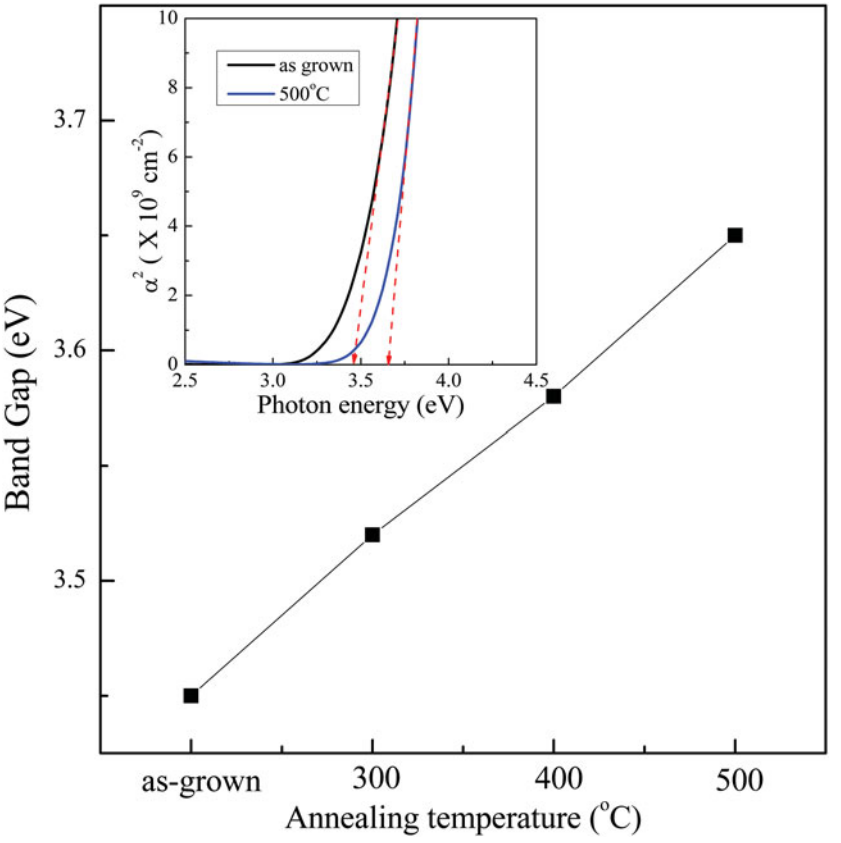

Figure 6. Optical band gap of ZTO films as a function of annealing temperature.

is increased after annealing process, and further increases with the increase of annealing temperature. This blue-shift of E_g can be interpreted by Burstein-Moss shift [18,19], due to the increase in the carrier concentration.

Conclusions

In summary, transparent semiconducting ZTO thin films with the thickness of about 100 nm were prepared by RF-magnetron sputtering techniques with powder target. Thermal annealing treatment at above 400 °C in vacuum ambient give rise to be crystallization of ZTO films, showing inverse cubic spinel structure with a preferred grain orientation in the (311) direction. The increasing annealing temperature leads to the increase in Hall mobility and electron concentration, resulting in the decrease of resistivity. Regardless annealing temperature, optical transmittances of about 80% in the visible range of the spectra were obtained for the all films. The optical band gap of the films increases with the increase of annealing temperature. From the results described above, it can be concluded that for the ZTO thin films prepared by radio-frequency sputtering with powder target, the annealing process at above 400 °C in vacuum for 1 hr is a good method to fabricate transparent semiconducting ZTO thin films.

References

[1] Tsao, S. W., Chang, T. C., Huang, S. Y., Chen, M. C., Chen, S. C., Tsai, C. T., Kuo, Y. J., Chen, Y. C., & Wu, W. C. (2010). *Solid-State Electron.*, *54*, 1497.
[2] Lim, W., Douglas, E. A., Norton, D. P., Pearton, S. J., Ren, F., Heo, Y.-W., Son, S-Y, & Yuh, J.-H. (2010). *Appl. Phys. Lett.*, *96*, 053510.
[3] Lee, J. S., Park, J.-S., Pyo, Y.-S., Lee, D.-B., Kim, E.-H., Stryakhilev, D., Kim, T.-W., Jin, D.-U., & Mo, Y. -G. (2009). *Appl. Phys. Lett.*, *95*, 123502.
[4] Kim, M., Jeong, J., Lee, H., Ahn, T., Shin, H., Park, J., Jeong, J., Mo, Y., & Kim, H. (2007). *Appl. Phys. Lett.*, *90*, 212114.
[5] Saji, K. J., Jayaraj, M. K., Nomura, K., Kamiya, T., & Hosono, H. (2008). *J. Electrochem. Soc.*, *155*, H390.
[6] Chiang, H. Q., Wager, J. F., Hoffman, R. L., Jeong, J., & Keszler, D. A. (2005). *Appl. Phys. Lett.*, *86*, 013503.
[7] Jackson, W. B., Hoffman, R. L., & Herman, G. S. (2005). *Appl. Phys. Lett.*, *87*, 1.
[8] Fortunato, E., Pereira, L., Barquinha, P., Rego, A., Goncalves, G., Vila, A., Morante, J., & Martins, R. (2008). *Appl. Phys. Lett.*, *92*, 222103.
[9] Gorrn, P., Holzer, P., Riedl, T., Kowalsky, W., Wang, J., Weimann, T., Hinze, P., & Kipp S. (2007). *Appl. Phys. Lett.*, *90*, 063502.
[10] Sato, Y., Kiyohara, J., Hasegawa, A., Hattori, T., Ishida, M., Hamada, N., Oka, N., & Shigesato, Y. (2009). *Thin Solid Films*, *518*, 1304.
[11] Satoh, K., Kakehi, Y., Okamoto, A., Murakami, S., Moriwaki, K. & Yotsuya, T. (2008). *Thin Solid Films*, *516*, 5814.
[12] Wasa, K. & Hayakawa, S. (1992). *Handbook of Sputter Deposition Technology - Principles*, Technology and Applications, Noyes Publications, New Jersey.
[13] Audronis, M., Kelly, P. J., Arnell, R. D., Leyland, A., & Matthews, A. (2005). *Surf. Coat. Technol.*, *200*, 1366.
[14] Nimisha, C. S., Rao, K. Y., Venkatesh, G., Rao, G. M., & Munichandraiah, N. (2011). *Thin Solid Films*, *519*, 3401.

[15] Chen, X., Guan, W., Fang, G., & Zhao, X. Z. (2005). *App. Surf. Sci.*, *252*, 1561.
[16] Fortunato, E., Barquinha, P., Goncalves, G., Pereira, L., & Martins, R. (2008). *Solid-State Electron.*, *52*, 443.
[17] Shin, H. J., Han, D. C., Choi, Y. C. & Lee, D. K. (2011). *Mol. Cryst. Liq. Cryst.*, *550*, 13.
[18] Burstein, E. (1954). *Phys. Rev.*, *93*, 632.
[19] Wu, W. F., & Chiou, B. S. (1994). *Semicond. Sci. Technol.*, *9*, 1242.